J. Geomag. Geoelectr., **46**, 39–57, 1994

GEOTAIL Energetic Particles and Ion Composition Instrument

D. J. WILLIAMS[1], R. W. MCENTIRE[1], C. SCHLEMM II[1], A. T. Y. LUI[1], G. GLOECKLER[2], S. P. CHRISTON[2], and F. GLIEM[3]

[1]*The Johns Hopkins University, Applied Physics Laboratory, Laurel, MD 20723-6099, U.S.A.*
[2]*The University of Maryland, College Park, MD 20742, U.S.A.*
[3]*Institut fuer DV-Anlagen, T.U. Braunschweig, Braunschweig, Germany*

(Received May 6, 1993; Revised October 15, 1993; Accepted October 25, 1993)

The Energetic Particles and Ion Composition (EPIC) instrument, flown onboard the GEOTAIL satellite, is designed to measure the characteristics of particle populations important to understanding the make-up and dynamics of the earth's geomagnetic tail. To do this, EPIC, a joint endeavor between the Technical University of Braunschweig (TUB), the University of Maryland (UM), and The Johns Hopkins University Applied Physics Laboratory (JHU/APL), is made up of five subassemblies: the Supra-Thermal Ion Composition Spectrometer (STICS) sensor, the STICS analog electronics, the Ion Composition System (ICS) sensor, the ICS analog electronics, and the Data Processing Unit (DPU). The STICS sensor provides ~4π angular coverage, composition and spectral observations, with charge state determination for all ions from 30 keV to 230 keV/e, and mass per charge measurements ≥7.5 keV/e. The ICS sensor provides flux, composition, spectra, and angular distributions over two polar angles of the elemental species protons through iron from ≥50 keV to 3 MeV along with angular distributions in one plane of electron fluxes >32 keV and >110 keV. The DPU provides the capability of numerous operating modes from which a small number will be selected to optimize data collection throughout the many phases of the GEOTAIL mission. To date the EPIC instrument performance has been very successful. In this paper we describe the instrument, its operation, and show some of our early results.

1. Introduction

The GEOTAIL satellite plays a major role in the International Solar-Terrestrial Physics (ISTP)-Global Geospace Studies (GGS) program. In this international effort to study the mass, momentum, and energy flow through the magnetosphere, GEOTAIL provides observations in one of the main magnetospheric storage and dissipation regions, the geomagnetic tail. Using an orbit adjust capability GEOTAIL will pursue the two general objectives of 1) exploring and studying the distant geomagnetic tail (out to distances of ~215 R_e), and 2) searching for the substorm initiation process in the ~8–30 R_e distance range.

Initial deep-tail explorations have been performed by the ISEE-3 satellite (see, e.g., papers in *Geophysical Research Letters*, Vol. 11, No. 10, 1984 and Lui, 1987). The discovery of large-scale plasma structures, called plasmoids, traveling rapidly tailwards (Hones *et al.*, 1984) has provided a strong central emphasis to the ISEE-3 deep-tail studies. For example, plasmoid-related features called traveling compression regions, the relation of plasmoid formation to near-earth substorm activity, and the role of energetic particle populations have been reported (e.g. Gloeckler *et al.*, 1984; Scholer *et al.*, 1984; Slavin *et al.*, 1984; Baker *et al.*, 1987; Murphy *et al.*, 1987; Richardson *et al.*, 1987). These ISEE-3 results show the distant tail to be a highly active plasma environment displaying a wide span of spatial structures and time scales and a strong connection to the inner magnetospheric regions where substorm activity is strong and thought to originate. In the deep tail portion of the mission, GEOTAIL instruments will provide both new exploratory observations and major extensions of these earlier ISEE-3 results.

EPIC provides measurements of ion spectra, ~4π angular distributions, ion composition for energies ≥10 keV/e and charge state ≥30 keV. Table 1 summarizes the main capabilities and characteristics of the EPIC instrument and Fig. 1 shows the ICS and STICS sensor boxes, their location on the periphery of the

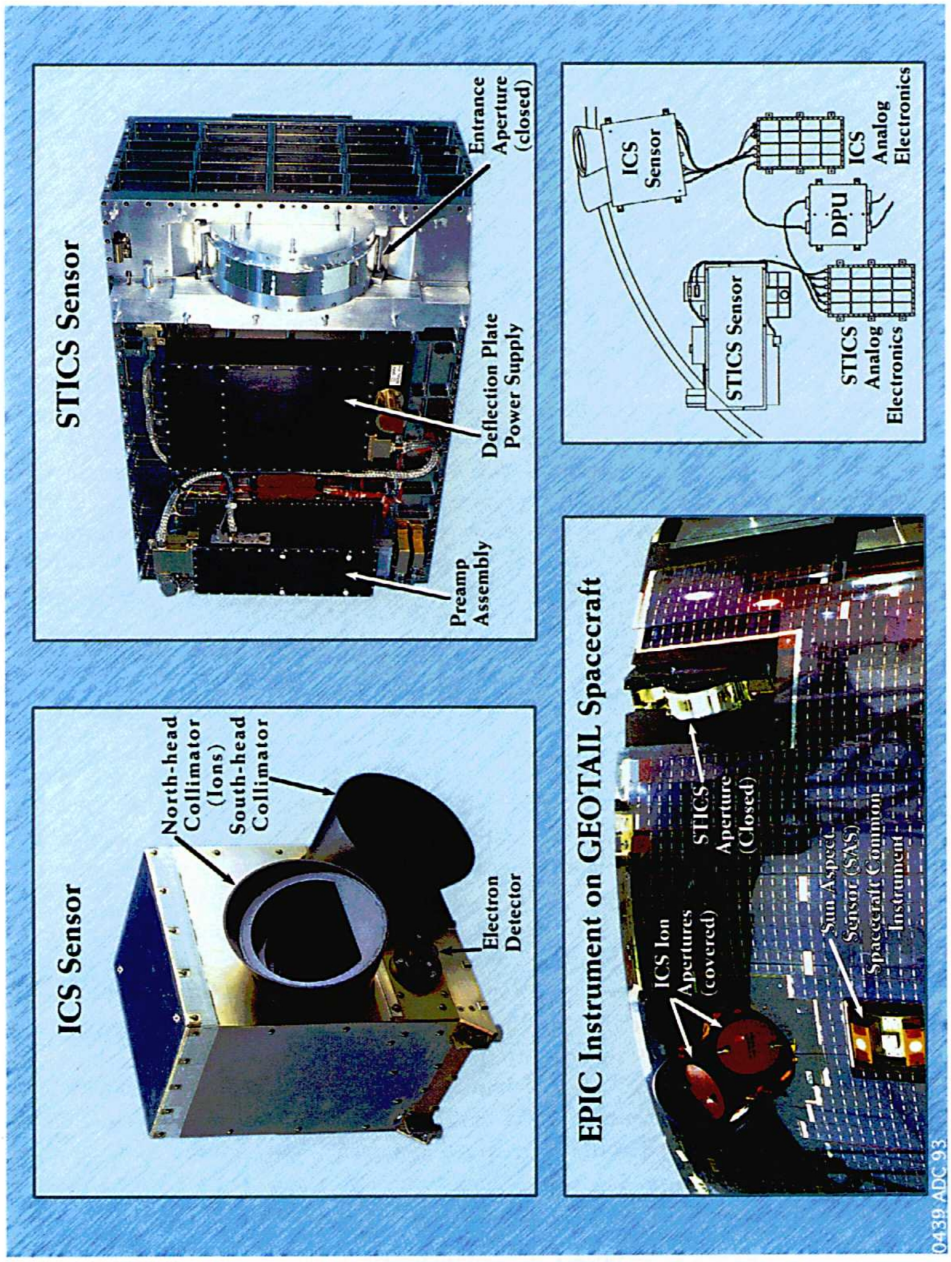

Fig. 1. The upper panels show the ICS and STICS sensor boxes, with thermal blankets removed. The lower left panel shows their projection through the solar cell panels at the periphery of the satellite. The lower right panel shows a schematic of the placement of all five EPIC subassemblies.

Table 1. EPIC summary table.

	STICS	ICS
Sensors	Electrostatic analyzer × time-of-flight × E	Time-of-flight × E
Energy range	7.5–230 keV/e (M/Q) 30 keV–230 keV/e (M and M/Q) $\Delta E/E = 5\%$	>10 keV (integral) ions >20 keV (velocity) ions >50 keV–3 MeV (M) ions >32 keV and >110 keV (integral) electrons
Ion species	H through Fe	H through Fe
Resolution:		
Mass	Resolves all major ion species	Resolves all major ion species
Charge	Charge states of major ion species	
Angular	6 equal 26.7° polar sectors (+80° to –80°) 16 equal 22.5° azimuthal sectors	2 equal 30° polar sectors (–38° to –8°; +8° to +38°*) (ions) 1 polar 60° sector (–30° to +30°*) (electrons) 16 equal 22.5° azimuthal sectors
Time	3 sec**/energy step 24 sec**/8-point spectrum	0.2 sec to 96 sec** (species dependent)
Geometry factor	0.05 cm^2 sr	<0.006 to 0.2 cm^2 sr (ions) 0.1 cm^2 sr (electrons)
EPIC S/C interfaces:		
Mass	Total mass 21.9 kg (including shielding, excluding cables)	
Power	14.6 W electronics, <10 W thermal	
Data rate	2560 bps	

*With respect to the spin plane.
**Assumes the nominal 3 seconds/spin.

Table 2. EPIC science team.

T. P. Armstrong	University of Kansas
S. P. Christon	University of Maryland
F. Gliem	Technical University of Braunschweig
G. Gloeckler	University of Maryland
R. Gold	JHU/APL
A. Hasegawa	Osaka University
F. Ipavich	University of Maryland
S. M. Krimigis	JHU/APL
L. J. Lanzerotti	Bell Labs.
A. T. Y. Lui	JHU/APL
R. W. McEntire	JHU/APL
C.-I. Meng	JHU/APL
K. Papadopoulos	University of Maryland
E. C. Roelof	JHU/APL
E. T. Sarris	Demokritos University of Thrace
T. Sato	University of Tokyo
D. J. Williams (P.I.)	JHU/APL

GEOTAIL satellite, and the placement of the five EPIC subassemblies. The 4π angular distributions assure that the necessary energetic particle measurements will be obtained independent of magnetic field direction and/or satellite orientation. The charge state measurements provide a means of identifying the source(s) for the particles seen throughout the tail as well as providing a unique marker in the tracking of particle populations through the magnetosphere. The large-geometric-factor composition measurements provide the capability of observing the behavior of the major particle groups even during periods of very low activity. In addition to the ion measurements, EPIC measures electron fluxes and angular distributions in one plane, mainly to provide an indication of field line topology, i.e., open or closed.

The EPIC data will allow the pursuit of many scientific studies throughout the 8–215 R_e distance range of GEOTAIL. General scientific objectives are to:

- determine of the source(s) of the ambient magnetotail energetic particle populations and their relative strengths as a function of time and position in the tail,
- determine the source(s) of ions in large-scale plasma structures such as plasmoids,
- study the formation region of plasmoids,
- evaluate the importance of the distant magnetotail as a determinant of or a result of magnetospheric dynamics,
- study the formation and dynamics of magnetospheric boundary layers such as the magnetopause, the low-latitude boundary layer, the plasma sheet boundary layer and the neutral sheet,
- evaluate the relative strengths of the ionospheric (including the plasmasphere) and solar wind sources,
- evaluate the importance of charge exchange, pitch angle diffusion, single particle motion, and energy diffusion as loss processes,
- evaluate the importance of single particle motion, collective motion, convection, and magnetic field driven drifts as transport mechanisms,
- evaluate the effectiveness of acceleration processes such as electrostatic electric fields, and induced electric fields (betatron and Fermi acceleration and other $\partial \boldsymbol{B}/\partial t$ effects).

The in-flight calibrations, certification of the data, and initial analyses are the responsibility of the EPIC science team shown in Table 2. However the key to the success of the ISTP-GGS-GEOTAIL missions will be the analysis of the combined data obtained by the suite of instruments carried by these satellites. The EPIC team looks forward to this long-planned opportunity to greatly extend our understanding of the earth's magnetosphere through joint studies with all participating scientists using the ISTP data set. The following sections of this paper describe the EPIC instrument, its operation, its flight performance, and early data returns.

2. Instrument Description

2.1 Instrument overview

The EPIC instrument consists of three major subsystems comprised of the five subassemblies shown in Fig. 1. The Supra-Thermal Ion Composition Spectrometer (STICS—made up of the STICS sensor and STICS analog electronics); the Ion Composition System (ICS—made up of the ICS sensor and ICS analog electronics); and the Data Processing Unit (DPU). Photographs of the two sensors individually, as they project from the GEOTAIL spacecraft, along with a diagram showing the unit placement on the spacecraft upper deck are given in Fig. 1. EPIC instrument parameters are summarized in Table 1.

2.2 ICS

The ICS sensor is composed of three separate heads. Two of the heads are essentially identical, and measure ion spectra and species composition. Each of these heads employs a collimator, an electron sweeping magnet, a motor-driven variable aperture, and both a time-of-flight (TOF) measurement and a silicon solid-state energy detector. The third head primarily measures electron fluxes and employs a collimator, a blocking foil, and an energy sensor. A dedicated electronics package, including shaping

amplifiers, discriminators, time-of-flight circuits, analog-to-digital converters (ADCs), valid-event logic, rate accumulators, and a low-voltage power supply (LVPS), is housed in the separate ICS Analog Electronics (IAE) box. The digital outputs from the IAE go to the common Data Processing Unit (DPU). A simplified schematic cross section of a single ICS TOF sensor and a block diagram of the ICS electronics are given in Figs. 2 and 3, respectively.

The electron detector collimator has a rectangular field-of-view 20 degrees wide in azimuth by 60 degrees in latitude, centered on the spin-plane. A 28,000 Å aluminum foil in front of the 500 μ thick ion-implant solid state detector stops ions less than 300 keV and determines the electron energy response of this detector, as given in Table 1.

The two nearly identical ion heads (north and south) use conical collimators made of graphite epoxy with anti-scattering baffles. The north (south) collimator is centered 23 degrees above (below) the spin-plane. The ion head collimators are followed by an electron sweeping magnet assembly with a central field strength of 740 gauss, designed to remove electrons with energy <200 keV from the field of view.

Following the sweeping magnet assembly, there is a variable aperture mechanism that has four commandable positions to alter both the telescope geometry factor and the minimum energy threshold. This was included to accommodate the large range in ion intensities and spectra expected throughout the orbital range of the GEOTAIL satellite. An open position provides no restriction to incoming particles. A second position inserts a 3940 Å thick Al/Lexan foil which raises the energy threshold for incoming ions without appreciably changing the geometry factor. The third position contains an identical foil preceded by a plate with 10 percent transmission. The fourth, a closed/calibrate position, fully blocks the aperture and contains a degraded alpha source for calibrating the TOF/energy telescope.

Following the variable aperture assembly, ions traverse a very thin (1900 Å thick) Al/Parylene front foil, travel a 6.4 cm TOF path and strike the back 300 mm^2 350 μ thick silicon surface barrier solid state detector (SSD), where residual ion energy is measured. Secondary electrons produced from the surfaces of both the front foil and the rear SSD are accelerated, reflected by an electrostatic mirror, and impact

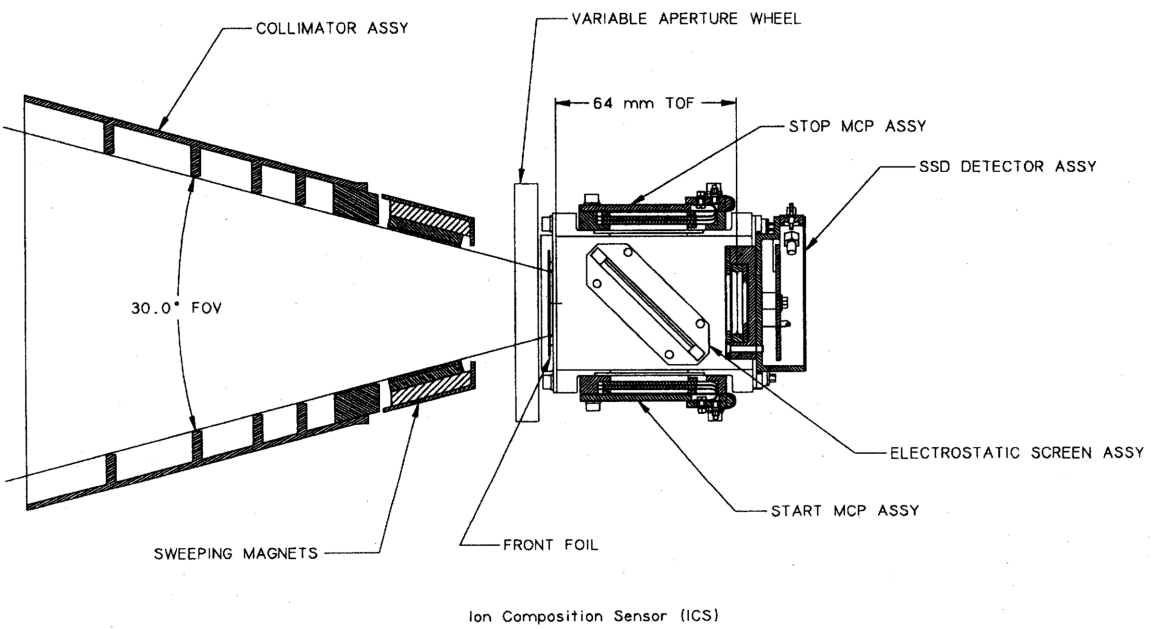

Fig. 2. A schematic diagram of one of the ICS Time-of Flight telescopes. Incident ions pass through the collimator, aperture, and front foil, and stop in the rear SSD. Secondary electrons from the surface of the front foil (or SSD) are accelerated into the inside of the head (which floats at 1000 V), reflected at the screen assembly, and mapped onto the start (or stop) MCP.

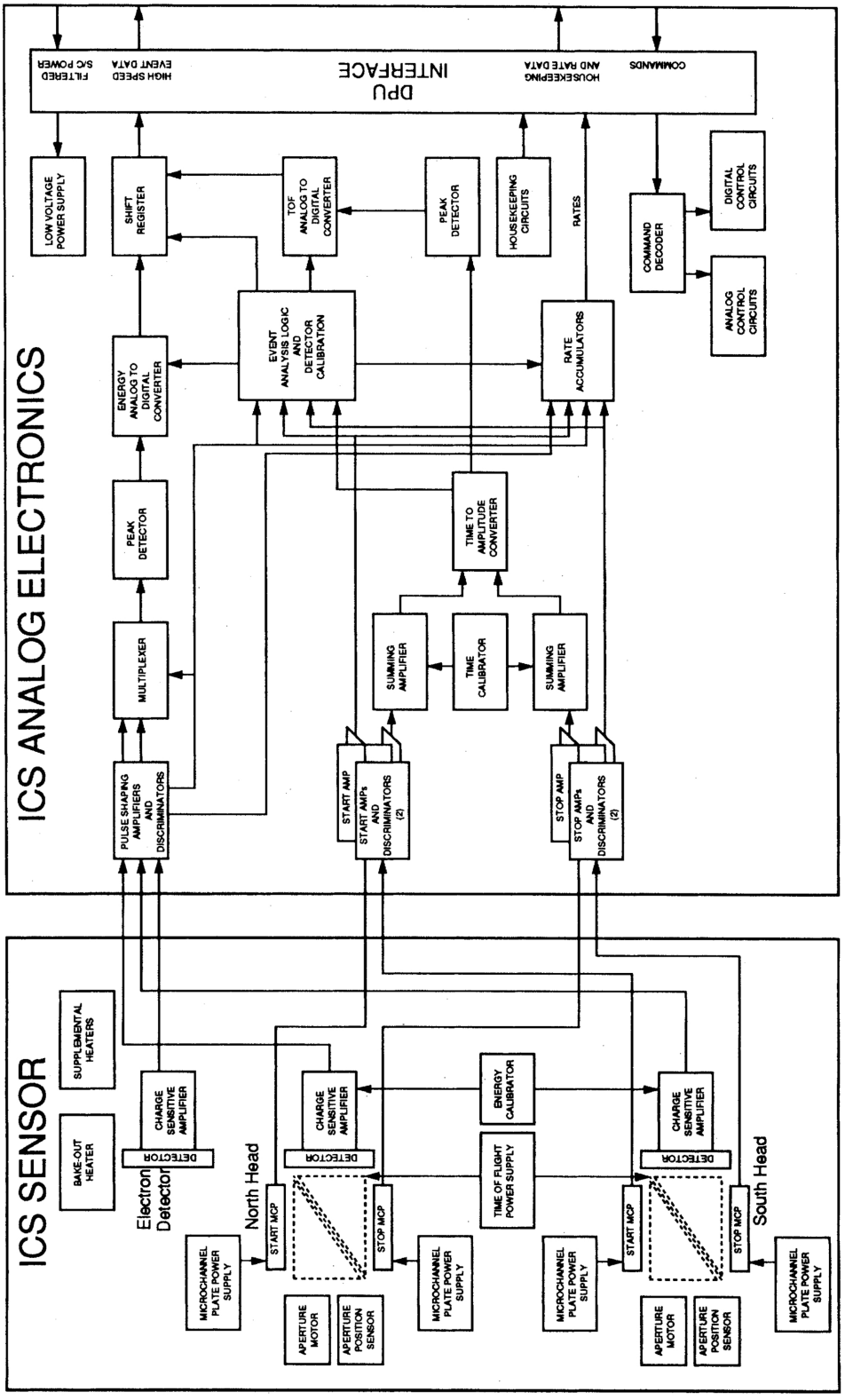

Fig. 3. EPIC Ion Composition System functional block diagram.

chevron-pair microchannel plate (MCP) detectors that provide, respectively, the start pulse and the stop pulse to the TOF electronics. Ion TOF is thus measured over the range of 2 to 100 ns. The ICS sensor package also contains five high voltage supplies—one for each MCP detector assembly, and one to provide electrostatic optics potentials for both ion heads. The ICS detector telescopes are thermally isolated, and operate at –10 to –20°C to reduce noise.

2.3 STICS

The STICS sensor contains an electrostatic ion E/Q analyzer, three time-of-flight/energy telescopes, TOF and deflection system high voltage power supplies, energy detector preamplifiers, and thermal control. The remainder of the analog electronics are located in the separate STICS Analog Electronics (SAE) box. As in the case for ICS, this was done primarily to reduce electronic heat dissipation in the sensor assembly. The digital outputs from the SAE are sent to the common DPU. A simplified schematic cross section of the STICS sensor and a block diagram of the STICS electronics are given in Figs. 4 and 5, respectively.

Particles enter the deflection system through a simple entrance aperture that includes a light trap. The deflection system consists of two concentric hemispherical shells of 107.75 mm mean radius, with a 4.50 mm gap and a deflection angle of 125 degrees. The polar acceptance angle is 159 degrees, centered on the spin-plane. Differential plate potentials range logarithmically between 600 and 20,000 volts, and are arranged in 32 possible steps that cover the entire E/Q range of the sensor (~8 to 230 keV/e). Deflection voltages normally change once per spacecraft spin (~3 seconds), and the sequence being used repeats every EPIC science record (SR), defined as 32 measured spins.

The deflection system is followed directly by the time-of-flight system. The three STICS TOF/energy telescopes each have a thin (~2 μg/cm^2) carbon conversion foil at the entrance of the TOF path. Secondary electrons are produced from the inner surface of the foil as the incoming ions pass through the foil. The secondary electrons within a particular TOF/energy telescope are guided by an electrostatic steering assembly to strike a chevron-pair MCP detector, producing a start pulse. The three start MCPs each have divided anodes, providing a latitudinal resolution of 26.5 degrees (six polar sectors). At the far end of each TOF system, the incoming ions strike a silicon surface barrier energy detector, providing a measure of residual ion energy and producing secondary electrons that are deflected to a stop MCP. The TOF system uses seven high voltage supplies: one for each MCP detector assembly (one start and one stop for each of the three TOF telescopes), and one to provide electron deflection potentials for all three telescopes. As with the ICS telescopes, the STICS head is operated at –15°C to reduce noise.

2.4 Analog electronics

The block diagrams of the ICS and STICS AE boxes are shown in Figs. 3 and 5, respectively. Energy signals coming from the charge sensitive amplifiers in the sensor (ICS or STICS) receive additional amplification, pulse shaping, and baseline restoration (to shorten recovery time) and are then routed to the Energy ADC, which performs a 10-bit analog-to-digital conversion when requested by the event analysis logic and sends the data to the DPU.

ICS uses two Start and two Stop channels of MCP pulse processing circuitry, and STICS uses six Start and three Stop channels. An appropriate Start signal causes the time to amplitude converter to begin a linear voltage ramp, and an appropriate Stop signal terminates the ramp, producing an amplitude that is held for the TOF ADC, which, just like the Energy ADC, performs a 10-bit analog-to-digital conversion when requested by the event analysis logic, and sends the data to the DPU. The event analysis logic uses coincidence conditions to determine the validity of an event, and triggers the ADC's. Transfer to the DPU of such fully-analyzed event data (digitized TOF and E for each event) is limited to $\approx 7 \times 10^4$ events/second for each of the STICS and ICS units. In the DPU this individual event data is processed and binned into, for example, species, E, and TOF science channels.

In addition each AE box contains rate accumulators—a series of 24-bit counters that accumulate singles rates from each detector in each sensor, and coincidence and anticoincidence rates useful in

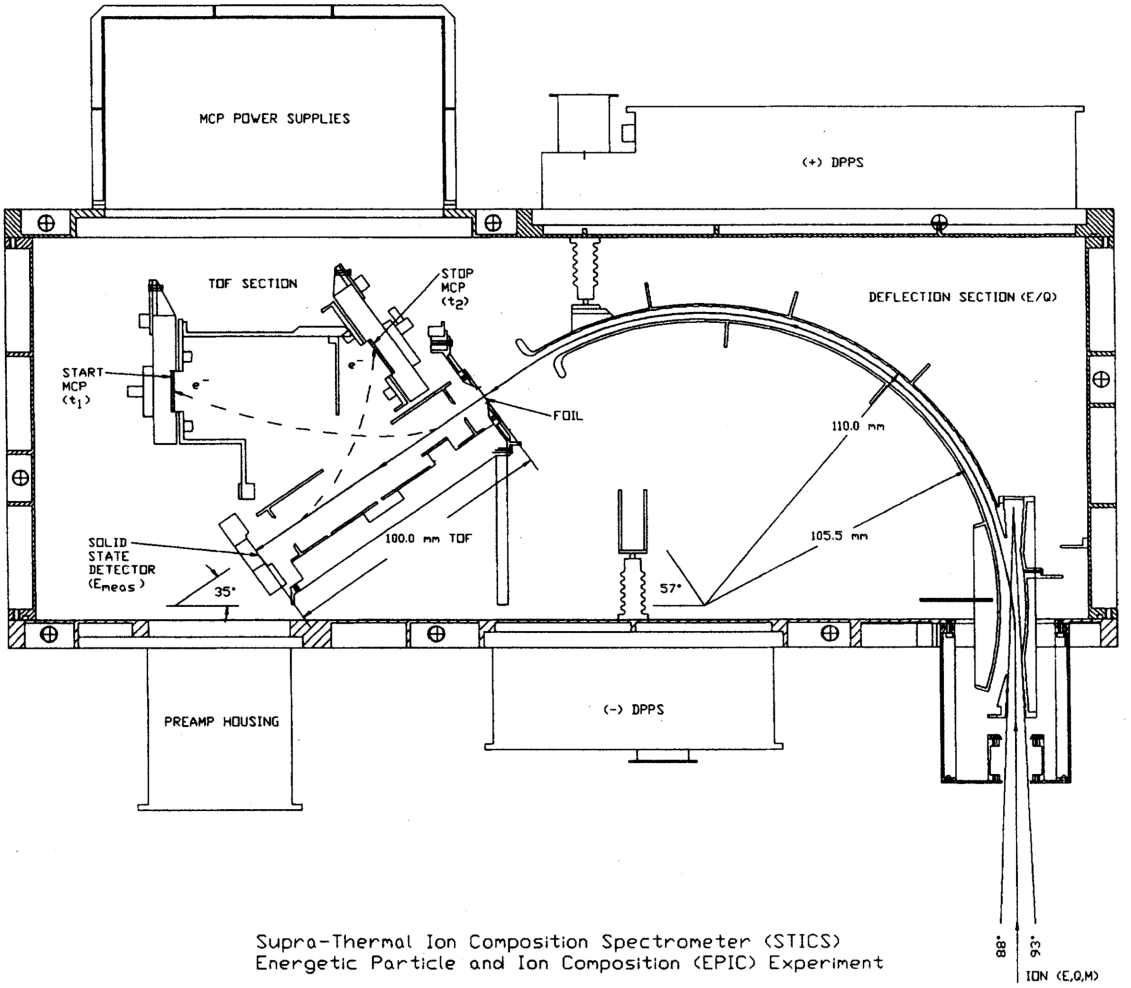

Fig. 4. Schematic diagram of the STICS sensor. This is a cut through the sensor in the s/c spin plane. Ions enter through the aperture, pass through the electrostatic E/Q analyzer, penetrate the TOF telescope front foil and stop in the back SSD, where their residual energy is measured. Ion TOF is measured using secondary electrons from the surface of the foil (or SSD), mapped to the start (or stop) MCP by electrostatic optics.

analysis of instrument performance. These counters are not subject to the same bus transfer limits, and can handle rates to $>10^6$ cps.

2.5 DPU

The DPU classifies measured particle events, tabulates event statistics (binning), formats telemetry, executes commands, collects instrument status information (housekeeping), and autonomously monitors key instrument health parameters for alarm conditions and provides safeing when limits are exceeded. It also provides the interface between the GEOTAIL satellite and the ICS and STICS subsystems. The DPU block diagram is shown in Fig. 6.

Event classification is performed by separate dedicated hardware for the ICS and STICS subsystems. For each event, processing for ICS involves determining the mass of the incident ion from the energy and TOF information sent to the DPU from the IAE, and summing the event into the correct mass, energy and TOF bins in memory. In addition a small number of events (eight/second) are selected (by a rotating

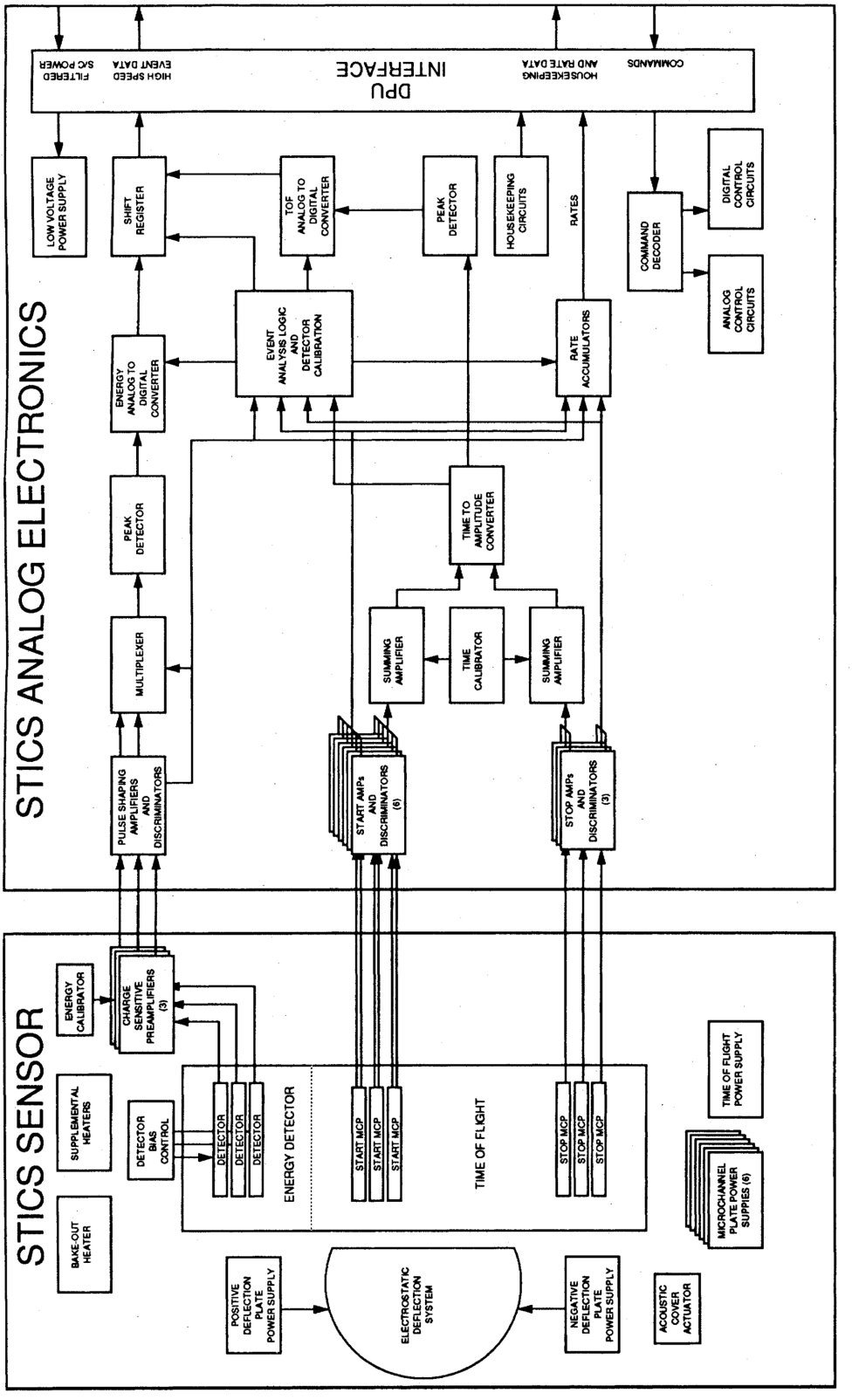

Fig. 5. EPIC STICS functional block diagram.

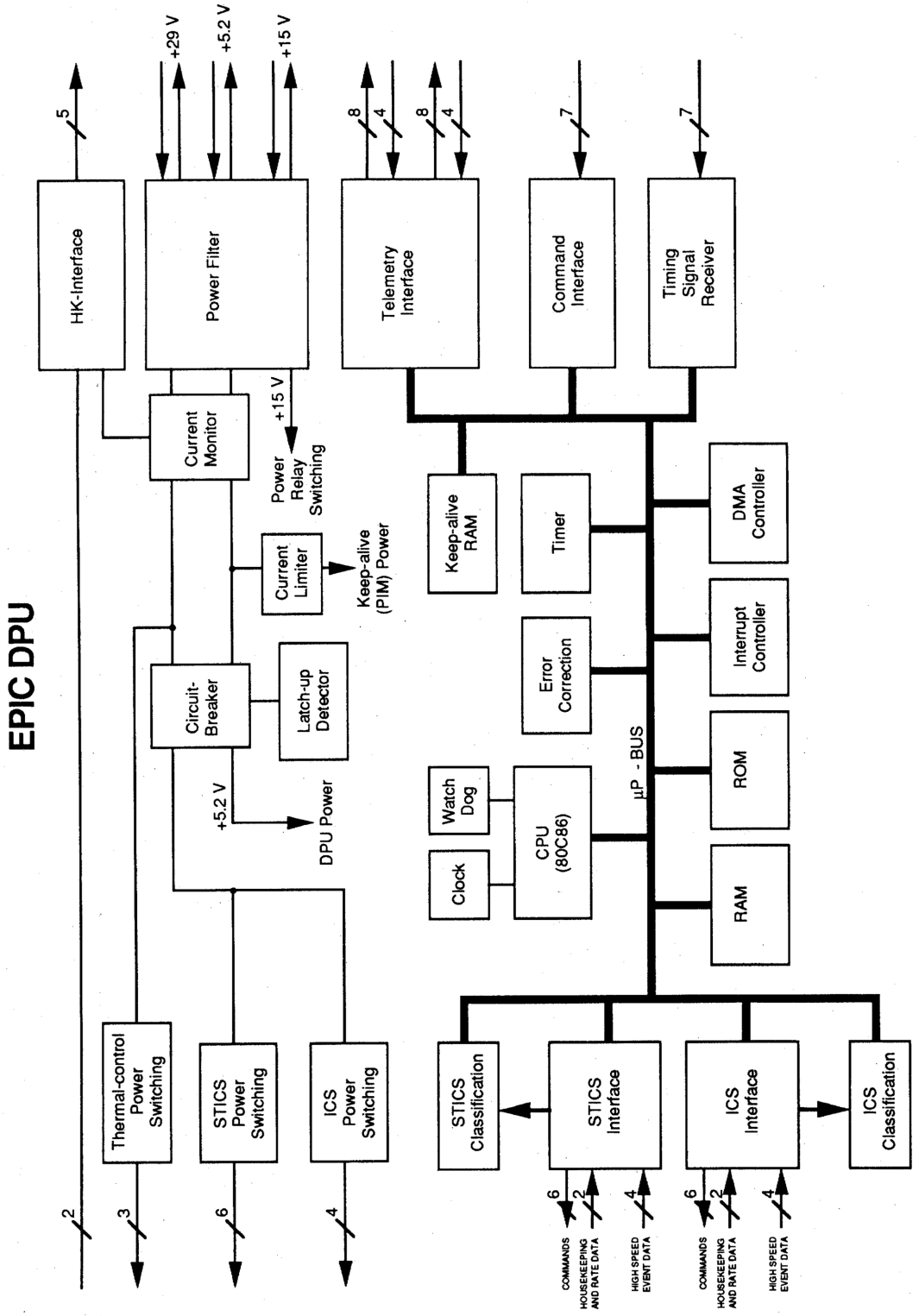

Fig. 6. Functional block diagram of the EPIC data processing unit.

priority system) to be transmitted to the ground as "PHA" events, with full TOF and E resolution, for more detailed analysis. The STICS processing also involves mass determination and event selection and binning, and additionally includes mass/charge calculations using TOF and energy/charge measurements. As maximum rates made direct calculation impossible, look-up tables are used to speed processing.

All binned data and PHA events are ultimately compressed, formatted, and sent to the S/C data system by the DPU, along with engineering and status parameters. In addition the DPU monitors a large number of dynamic housekeeping parameters and compares them to chosen alarm limits. If a value is outside a limit, the DPU acts to safe and/or recover from the condition. DPU operation is monitored by circuit latch-up and watchdog time-out detectors. The watchdog time-out monitors operating system errors that are caused primarily by bit-upsets, and the circuit latch-up detector looks for small (soft) and large (hard) latch-up conditions in segments of the DPU hardware. Triggering either condition will cause the sensor power to be turned off, the DPU power to be cycled, and optionally, the instrument to be re-configured back to its previous operational state.

3. Operational Modes

3.1 Instrument data structure

EPIC science data contains 960 bytes of data each spacecraft spin (3 seconds nominal). Of these ICS is normally allocated 360 bytes and STICS 576 bytes, with 24 bytes for status, etc.

The ICS data is primarily 16-sector rate channels, which are accumulated in the DPU for 1, 2, 16, or 32 spins (32 spins is one complete EPIC science record (SR), nominally 96 seconds). Rate channel coverage in TOF-E space is shown in Fig. 7. For each ion head there are 16 logarithmically distributed energy channels (E1–E16) covering the range of incident energies (for protons) of 46–3000 keV, 16 logarithmically distributed TOF channels (covering the TOF range of 2–100 ns), and 36 mass (species) channels. The mass channels are divided into 4 groups that are further divided by energy range: 10 channels each for Protons (P1–10), Helium (He1–10), and Mediums (M1–10, including primarily the

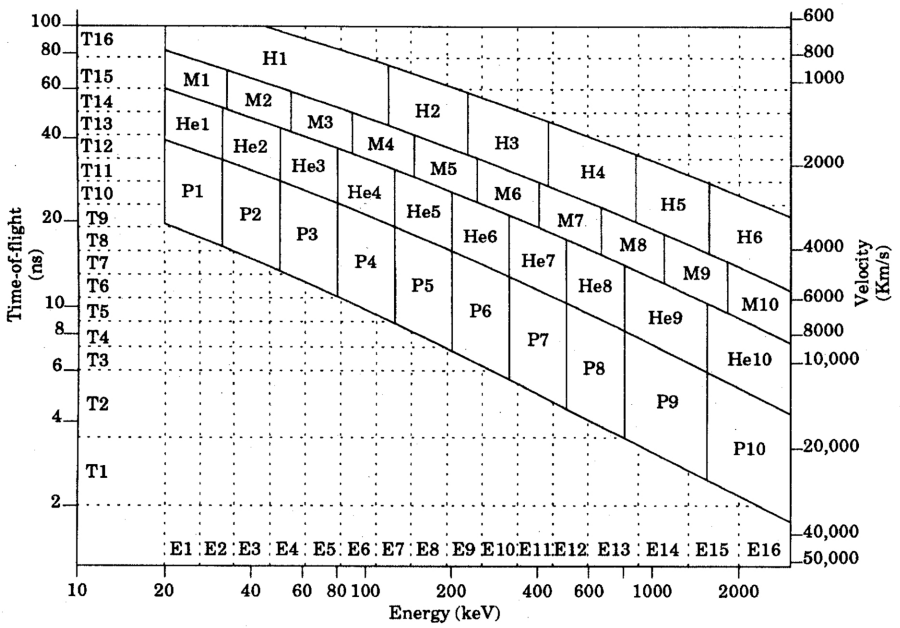

Fig. 7. Location of the 36 ICS species channels in the space of measured TOF vs. measured energy. In addition the location of the 16 single-parameter TOF (energy) channels is shown on the vertical (horizontal) axis.

carbon, nitrogen, oxygen group), and 6 channels for Heavies (H1–6, primarily the silicon group and iron). Incident energy passbands for these channels are shown in Table 3. The passbands shown for the M channels are for oxygen, and those for the H channels are for iron.

Table 3. EPIC/ICS rate channel passbands.

Channel name	Energy range (KeV)	Channel name	Energy range (KeV)	Channel name	Energy range (KeV)
P1	46–58	He1	54–70	M1	166–187
P2	58–77	He2	70–96	M2	187–222
P3	77–107	He3	96–135	M3	222–275
P4	107–155	He4	135–194	M4	275–360
P5	155–228	He5	194–281	M5	360–495
P6	228–342	He6	281–408	M6	495–700
P7	342–522	He7	408–595	M7	700–1016
P8	522–815	He8	595–890	M8	1016–1520
P9	815–1560	He9	890–1630	M9	1520–2315
P10	1560–3000	He10	1630–3055	M10	2315–3565
H1	400–620	H3	840–1200	H5	1770–2730
H2	620–840	H4	1200–1770	H6	2730–4400

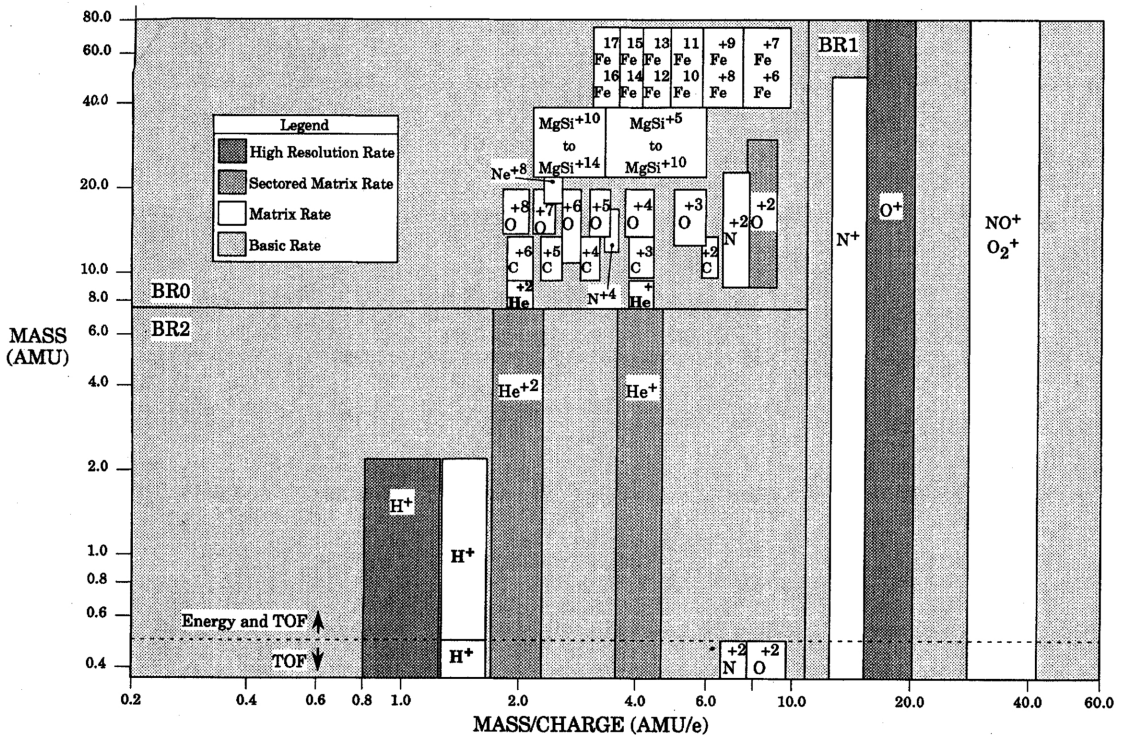

Fig. 8. STICS rate channel coverage in mass and mass/charge space. Shaded regions show the HR, SMR, BR and MR groups.

3.2 STICS

The STICS rate channels are transmitted every spin, and are composed of channels with angular resolution ranging from 3D to omnidirectional. The STICS channel coverage in mass and mass/charge space is shown in Fig. 8. Sectored rate channels consist of two High Resolution (HR) rate groups, three Sectored Matrix Rate (SMR) groups, and three Basic Rate (BR) groups. The HR groups contain full directional (6 polar × 16 longitudinal sectors) accumulations on two species; typically H^+ and time-shared O^+ or front MCP singles rates. The SMR groups contain partial directional (3 polar × 8 longitudinal sectors) accumulations on three ion species; typically He^+, He^{++}, and O^{++}. The BR groups contain partial directional information (3 polar × 8 longitudinal sectors) that cover the three PHA priority ranges. There are also 30 Matrix Rate (MR) channels, 21 detector accumulator rate channels, and 13 diagnostic rate channels, all of which are omnidirectional, and 47 PHA events/spin.

3.3 Operational modes

There are a large number of possible operational modes for EPIC involving permutations of: different angular and temporal resolution in sampling rate channels (and different thresholds/geometry factors for ICS); the definition of what the DPU considers a valid event (a coincident valid energy measurement and valid TOF measurement, or only one of these two, etc.); stepping rates and levels for the STICS E/Q electrostatic analyzer; reallocation of bit rates between ICS and STICS; calibration modes; and a number of other possibilities. These features are intended to provide great flexibility if needed to maximize science return or respond to operational requirements. However, to assure data analysis continuity, we intend to operate in only a small number of standard modes, selected for mission phase and orbital position.

4. Instrument Performance and Data Analysis

4.1 Calibrations

Prelaunch calibrations for both the ICS and STICS sensors were carried out at the NASA GSFC accelerator facility. Beams of ions of all of the major species and many different energies and charge states were input to the sensors, and instrument angular response and efficiency as a function of energy and species was determined.

4.2 Flight operations

The initial EPIC low voltage turn-on in orbit occurred on July 27, 1992, three days after the Geotail launch. Each subsystem was checked out and the ICS and STICS apertures were opened. All spacecraft high voltage subsystems (including the 14 EPIC HVPS's) were checked out in August, and following initial lunar swing-by and spacecraft thruster firings, EPIC was turned on for full science operations on September 29. Both ICS and STICS sensors have been operating well ever since, except for brief periods when high voltages are turned off to prevent possible problems during Geotail thruster firings.

As of this writing EPIC has been in full science operation for four deep-tail orbits. The normal operational mode has been with the STICS electrostatic analyzer stepping in voltage once every 3 seconds, in a repeating pattern of 8 steps covering incident ion energies from 9.4 to 212 keV/e. ICS is normally in its fully-open aperture position, but operates under an autonomous adaptive aperture control algorithm that monitors the front microchannel plate (start channel) counting rate, and changes to more restrictive aperture settings if the rates increase to unacceptably high levels. This occurs due to normal foreground rates occurring near perigee, and elsewhere in orbit only for very large events. The front microchannel plate rates in both ICS telescopes are sensitive to scattered sunlight in three (out of the 16) sectors centered on the sun, but coincidence requirements assure that solar contamination is not seen in any of the energy channels or species rate channels.

There are two sources of timely information on EPIC performance. The primary route is the Quick Look (QL) data from the first hour of each Geotail tape dump. These data are electronically transferred to APL each day, processed, and summarized for every science channel and all 343 engineering

housekeeping values. Daily review of this data, and of less frequent electronic calibration cycles, monitors both instrument health and sensor performance. The second route, used mainly at times of transmission of commands to EPIC, is an electronic link between ISAS and the EPIC ground support equipment (GSE) computer at APL, providing visibility into the complete EPIC data stream in real time. For example, the efficiency of each EPIC microchannel plate detector is monitored using QL data, and as fluence through each plate increases, bias voltages must occasionally be raised to maintain constant gain. When any commands are sent to EPIC the downlink data is monitored in real time, command loads received by the instrument are validated before execution, and instrument response is confirmed after command execution.

4.3 Data flow and processing

The primary route for scientific data to the EPIC team is via the ISTP Central Data Handling Facility (CDHF) (Fig. 9) which combines Geotail real-time and recorder playback data to create a nearly continuous Level Zero (L0) record of the original instrument telemetry. This data, which for EPIC is roughly 28 MBytes per day, is then distributed on magnetic tape to the EPIC team on average two weeks after its collection. At the team processing facility at the JHU/APL the data is then decommutated and synchronized to construct Level One (L1) instrument data files. This L1 data includes time and quality flags and spacecraft ephemeris and attitude, and is the primary EPIC archive. L1 data serves as the basis for all analytic study at APL and the co-investigator facilities.

To provide the scientific community with timely views of scientific conditions, the CDHF will regularly process L0 files to create key parameter (KP) survey data for each Geotail instrument. Each team designs the software which creates these KPs and delivers the resultant programs to the CDHF for use in routine production. The EPIC KP data files contain fluxes of ions and electrons, ion composition, and anisotropies.

4.4 Data analysis

The EPIC L1 files are created on the EPIC RDAF (a VAX station 4000/90). A set of standard science

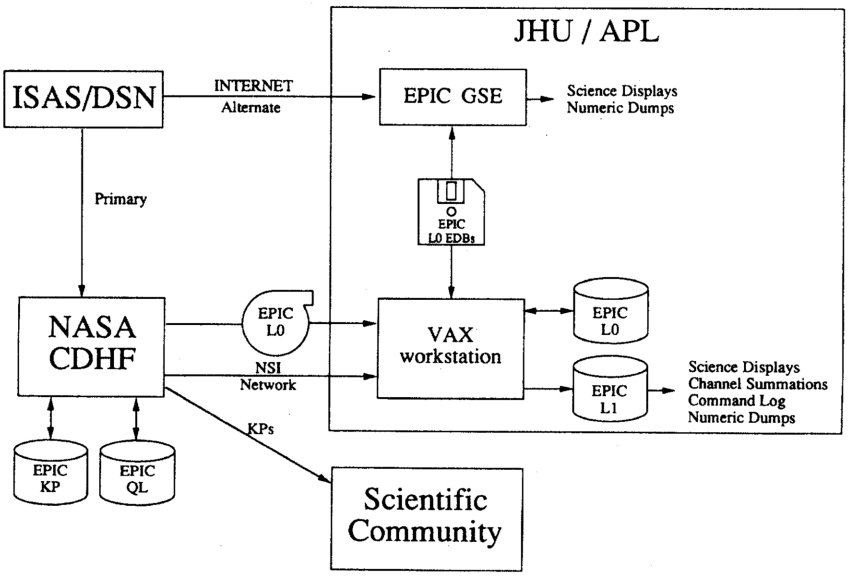

Fig. 9. EPIC data flow schematic. The primary source of EPIC scientific data is tape-play-back data processed at the ISTP CDHF, but during s/c operations a real-time route exists via an Internet link between APL and ISAS.

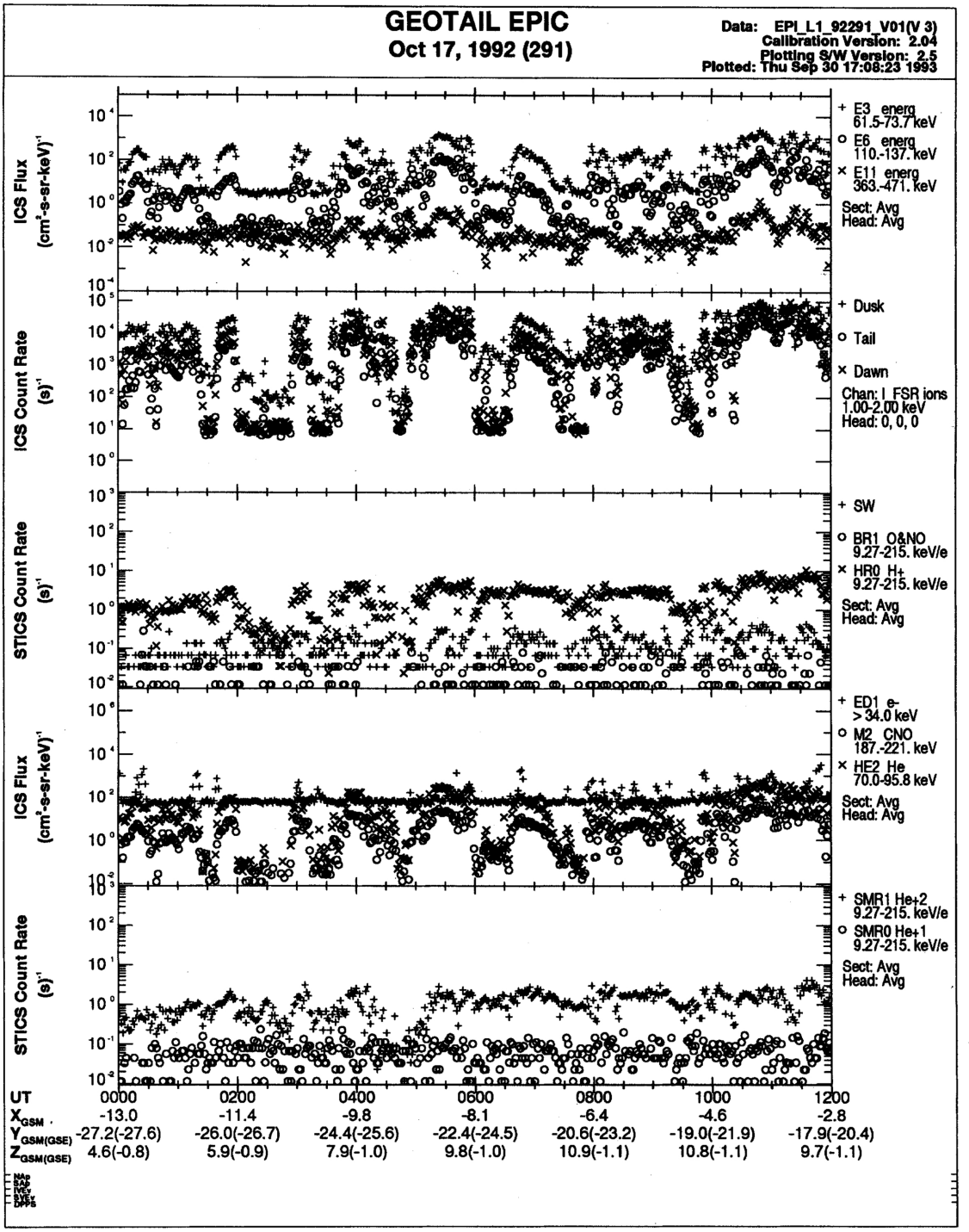

Fig. 10. A standard EPIC summary line plot. Such plots are generated to cover the entire mission. The top panel shows three ICS Energy channels (averaged over all directions and both ICS heads); the second panel shows counting rates for the front MCP (essentially all ions ≥10 keV) in the ICS North head in three different look directions; the third panel shows rates for three STICS species channels (averaged over energy and direction); the fourth panel contains ICS electrons and two species channels; and the last panel shows the two charge states of helium from STICS.

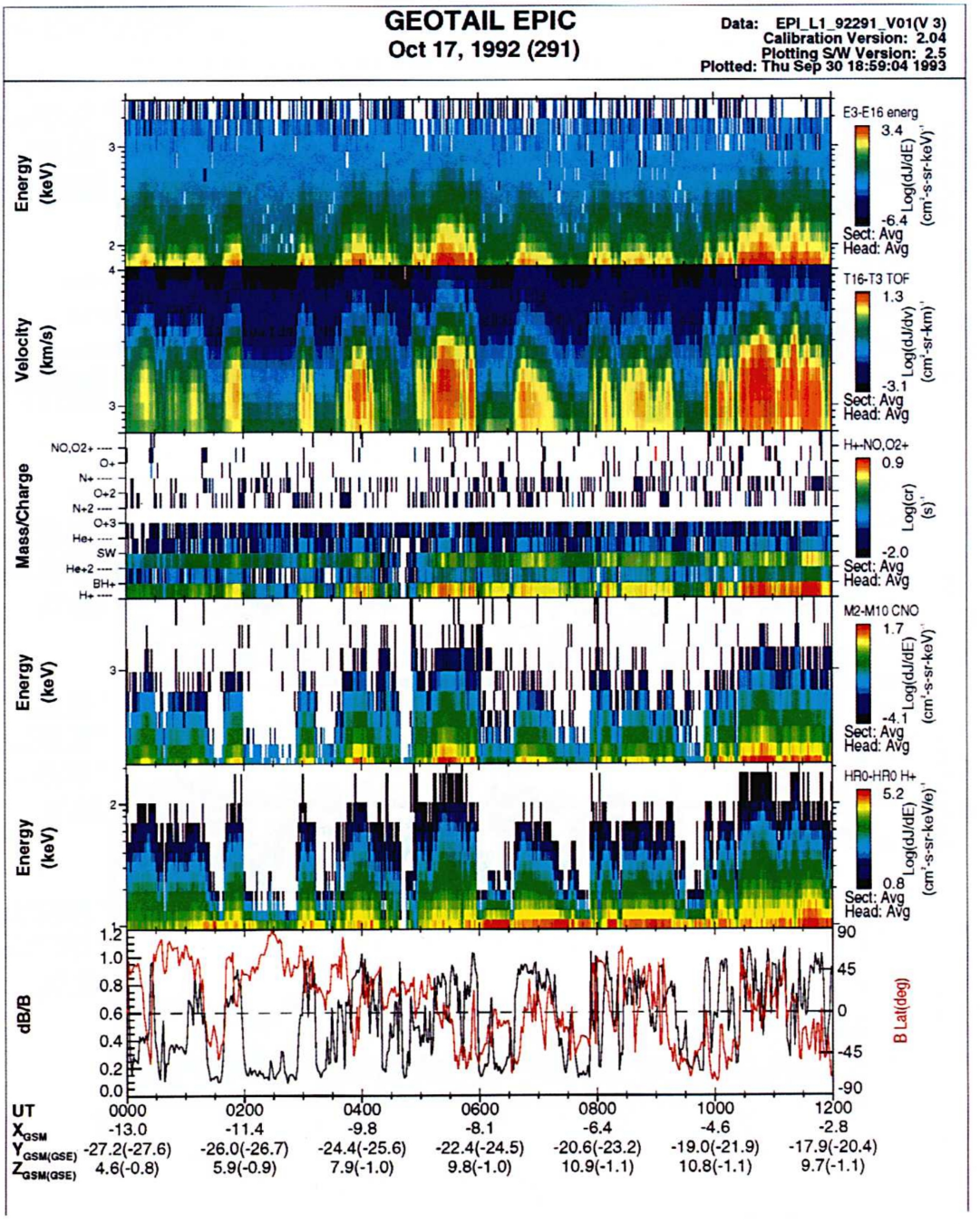

Fig. 11. A standard EPIC summary spectra plot. In addition to the summary line plot, a series of different 12-hour color summary plots such as this are generated for the entire mission for science overview. In this figure the first two panels contain omnidirectional energy (velocity) spectra derived from the ICS Energy (TOF) rate channels; the next contains a mass/charge composition summary (integrated over the STICS energy range). The fourth and fifth panels contain CNO spectra from the ICS Medium channels and low energy proton spectra from STICS. The last panel contains magnetic field latitudinal direction and variance (courtesy of Prof. Kokubun and the MGF team).

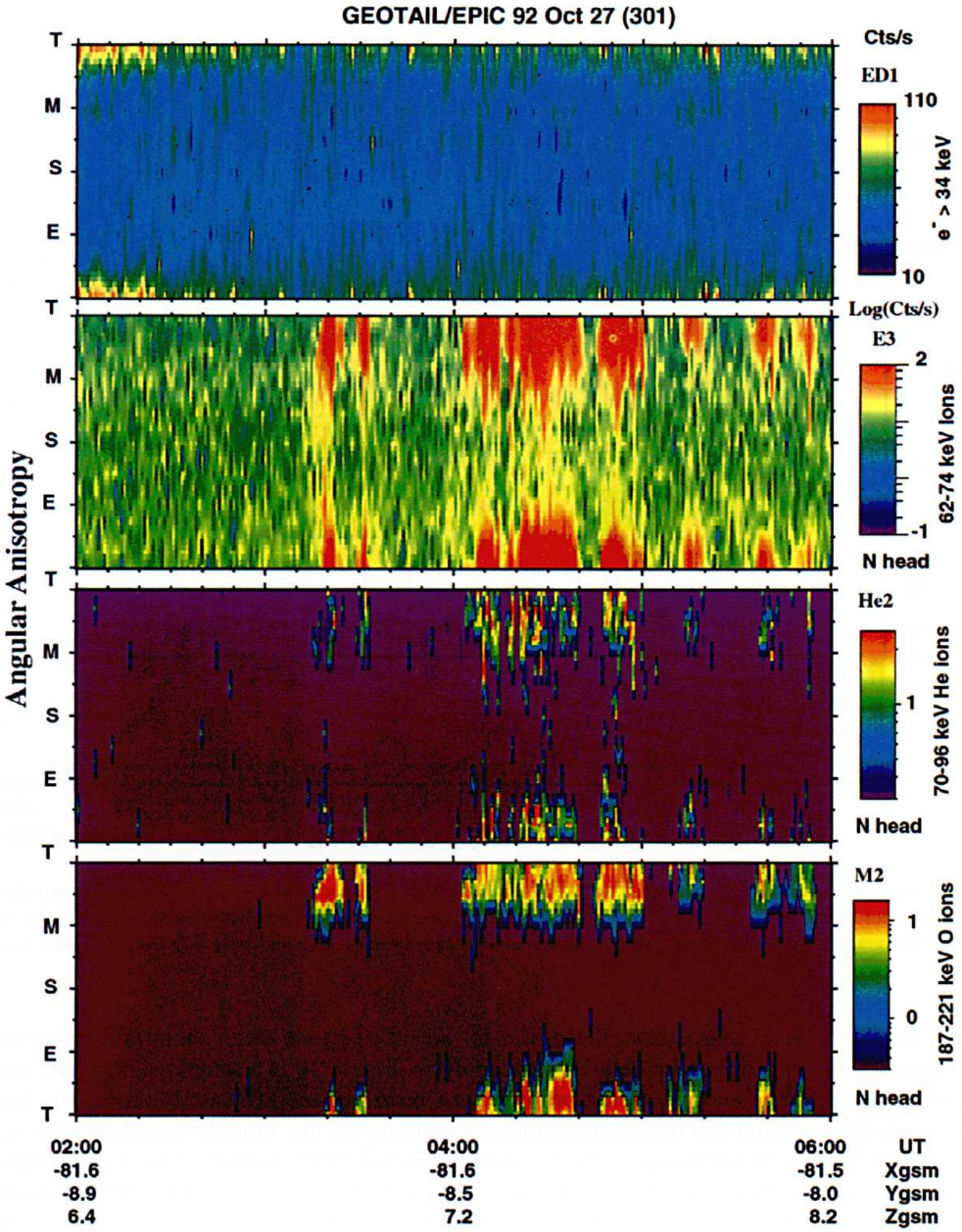

Fig. 12. Angular anisotropies for four ICS channels for a 4 hour period on October 27, 1992. The panels show in order electrons, the E3 ion channel, and the He2 and M2 species channels. The directions on the vertical axis represent streaming toward the Tail, Evening, Sun and Morning.

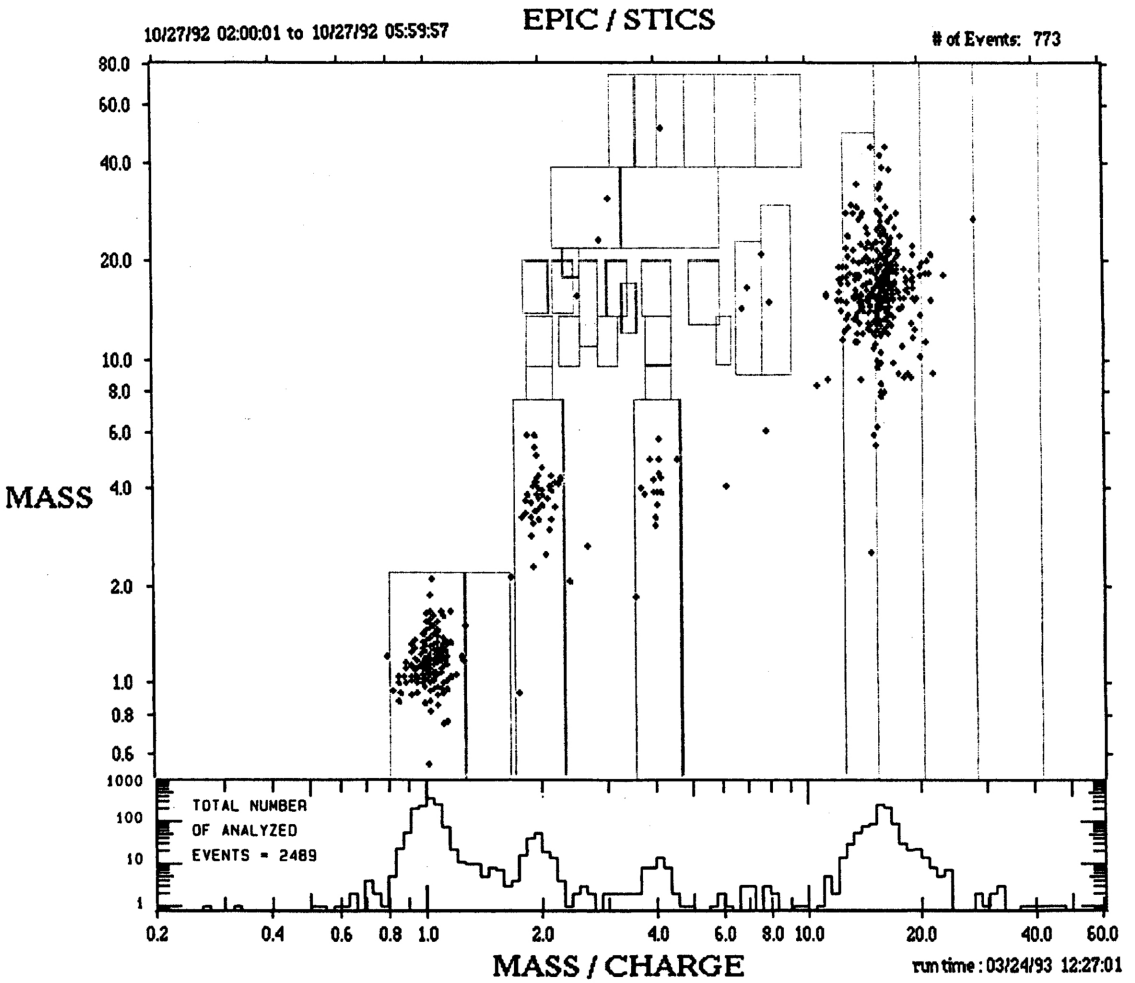

Fig. 13. Mass vs. mass/charge distribution seen by STICS for the same time period as in Fig. 12. The top part shows PHA events for which both M and M/Q were determined (this requires three-parameter measurements—E/Q, TOF, and E), while the bottom histogram plots just the M/Q distribution, and also includes events for which only E/Q and TOF were measured.

summary plots are then prepared from these files for all time periods received, both for overview and survey purposes and to guide more detailed data analysis. Figure 10 is a sample survey line plot for a moderately active period inbound during orbit 5; the Geotail spacecraft was skimming the boundary between the magnetosheath and the magnetosphere, including the low latitude boundary layer (LLBL). Numerous transitions between these regions are seen in selected EPIC channels. This is an example of the many times in which a great deal of energetic particle activity is seen in the EPIC energy ranges at the Geotail location. Figure 11 is an example of another type of standard survey plot. It shows energy and time-of-flight (velocity) spectra for all ions and for several species, a mass/charge composition summary, and magnetic field latitudinal direction and variance (courtesy of Prof. Kokubun and the MGF team), for the same period covered by Fig. 10.

Such combinations of line plots and color spectrograms provide excellent overviews into the EPIC data. However, much of the Geotail physics will be derived from high resolution studies of individual events. Figure 12 is drawn from one such study, in which the anisotropies of energetic electrons, 62–74 keV ions (primarily protons), 70–96 keV helium, and 187–221 keV oxygen ions seen by the ICS head are

displayed for an energetic event observed in the deep tail. The elemental and charge state composition seen by the STICS head for this event is given in Fig. 13, clearly showing the dominance of singly charged oxygen over higher charge states of oxygen ions, indicating a strong ionospheric source, while both charge states of helium are seen.

The EPIC instrument heads combine to give a combination of large geometry factor, large dynamic range, and excellent energy, charge state, and species resolution—well suited to the diverse space plasma regimes covered by the Geotail mission. EPIC flight data shows the distant magnetotail to be a very dynamic region, with distinctive variations in energetic ion flux, composition, and anisotropy. Scientific analysis of this excellent data set is now well underway.

The successful construction, test, and launch of the EPIC instrument has required the continuing efforts of many dedicated professionals. Space does not permit the recognition of everyone connected with the EPIC over the past decade. However, with apologies to inadvertent omissions, we wish to thank and acknowledge those many people who had major and/or continuing responsibilities in the EPIC effort. The following major contributors, exclusive of the authors of the present paper and those named therein, are listed with their organizational affiliation: B. Andrews, C. Eckler, M. Grimes, S. Jaskulek, E. Keith, D. Mehoke, S. Nylund, S. Purwin, N. Rothman, L. Suther, J. Tarr, R. Thompson, B. Tossman, S. Vernon, all from The Johns Hopkins University Applied Physics Laboratory; J. Cain, R. Cates, A. Galvin, R. Lundgren, J. Rossano, E. Tums, F. Wire, all from the University of Maryland; A. Hestermeyer and W. Wiewesiek from the Technical University of Braunschweig; A. Nishida and K. Uesugi from the Institute for Space and Astronautical Sciences; and S. Brown from the Goddard Space Flight Center. In addition we wish to acknowledge the exceptional efforts of the Institute for Space and Astronautical Sciences post-launch team in helping us through the instrument turn-on and check-out sequences. In particular H. Hayakawa, T. Mukai, M. Nakamura provided invaluable assistance. Thanks to all of you who have helped make the EPIC such a successful effort to date. This work was supported by a National Aeronautics and Space Administration contract to The Johns Hopkins University Applied Physics Laboratory under the Department of Navy Task IAF; Contract N00039-91-C-001.

REFERENCES

Baker, D. N., R. C. Anderson, R. D. Swickl, and J. A. Slavin, Average plasma and magnetic field variations in the distant magnetotail associated with near-Earth substorm effects, *J. Geophys. Res.*, **92**, 71–81, 1987.

Geophysical Research Letters, Vol. 11, No. 10, ISEE-3 Distant Tail Results, 1027–1105, 1984.

Gloeckler, G., M. Scholer, F. M. Ipavich, D. Hovestadt, B. Klecker, and A. B. Galvin, Abundances and spectra of suprathermal H^+, He^{++} and heavy ions in a fast moving structure (plasmoid) in the distant geotail, *Geophys. Res. Lett.*, **11**, 603–606, 1984.

Hones, E. W., Jr., D. N. Baker, S. J. Bame, W. C. Feldman, J. T. Gosling, D. J. McComas, R. D. Zwickl, J. A. Slavin, E. J. Smith, and B. T. Tsurutani, Structure of the magnetotail at 220 R_e and its response to geomagnetic activity, *Geophys. Res. Lett.*, **11**, 5–7, 1984.

Lui, A. T. Y. (editor), *Magnetotail Physics*, 433 pp., Johns Hopkins University Press, Baltimore, MD, 1987.

Murphy, N., J. A. Slavin, D. N. Baker, and W. J. Hughes, Enhancement of energetic ions associated with traveling compression regions in the deep geomagnetic tail, *J. Geophys. Res.*, **92**, 64–70, 1987.

Richardson, I. G., S. W. H. Cowley, E. W. Hones, Jr., and S. J. Bame, Plasmoid-associated energetic ion bursts in the deep geomagnetic tail: Properties of plasmoids and the post-plasmoid plasma sheet, *J. Geophys. Res.*, **92**, 9997–10,013, 1987.

Scholer, M., G. Gloeckler, D. Hovestadt, B. Klecker, and F. M. Ipavich, Characteristics of plasmoid-like structures in the distant magnetotail, *J. Geophys. Res.*, **89**, 8872–8876, 1984.

Slavin, J. A., E. J. Smith, B. T. Tsurutani, D. G. Sibeck, H. J. Singer, D. N. Baker, J. T. Gosling, E. W. Hones, Jr., and F. L. Scarf, Substorm associated traveling compression regions in the distant tail: ISEE-3 geotail observations, *Geophys. Res. Lett.*, **11**, 657–660, 1984.